Optical Microscope-Based Spectroscopy of Metal Nanostructures

Lara Backer

Michael Caverley

Project Sponsors:

Dr. Jeff Young

Dr. Georg Rieger

Group 1208

Engineering Physics 459

The University of British Columbia

2 April 2012

Executive Summary

A quantum dot is a piece of semiconductor material which has special electronic properties due to the fact that the quantum dot's electron wave function is confined in three dimensions to nanometer scale dimensions which are comparable to the wavelength of the electron's wave function. Optical experiments, which investigate quantum dots, are difficult to develop because of the small size scales encountered, causing low signal-to-noise ratio in measured data.

In this project, a LabVIEW control system was developed for an existing Nanopositioner apparatus, which consists of an optical microscope that focuses light on to a sample placed on a stage moving in three dimensions. Coherent forward scattering imaging methods were used to create images of the sample while the stage was moved. The control system locates the center of a region delimited by circular metallic reference markers 100 μm in diameter, where nanoparticles to be scanned were placed using an atomic force microscope. Piezoelectric actuators are used to move the stage with sub micron accuracy in order to image nanoparticles on the order of 50 nm. This control system and apparatus will allow the sponsors to further their research, which ultimately has applications in both optics and quantum information processing.

This project was sponsored by Dr. Jeff Young and Dr. Georg Rieger from UBC Physics and Astronomy in the Photonics and Nanostructures Laboratory. The control system and testing to obtain a reasonable scattered light signal from nanoparticles were completed by Lara Backer and Michael Caverley.

Table of Contents

List of Figures

List of Tables

1 Introduction

This report summarizes the work completed on the Nanopositioner apparatus at the UBC Photonics and Nanostructures Laboratory. The Nanopositioner apparatus will allow the researchers to investigate the optical properties of nanoparticles, ultimately allowing them to analyze the effects of placing nanoparticles in close proximity to quantum dots in optical cavities.

1.1 Quantum Dots

A Quantum Dot is a nanometer sized semiconductor crystal that has engineer-able optical properties. The emission spectrum is directly related to the size of the quantum dot. This occurs because the electrons inside the quantum dot are confined in such a way to create an energy band gap structure in between the continuous band gap structure in bulk semiconductor and the discrete band gap structure in single molecules. Due to the intermediate nature of the band gap spacing, the band gaps change depending on the size of the quantum dot and since the band gap structure determines the emission spectrum, the emission spectrum also depends on the size of the quantum dot. This property is useful because quantum dots can be fabricated with different spectra by only changing the size of the quantum dot and not the material the quantum dot is made of.

Our sponsors, Dr. Jeff Young and Dr. Georg Rieger, were interested in coupling resonant optical frequency oscillations of electrons in 5nm diameter PbSe nanocrystals, into optical circuits etched into the 200 nm top layer of a silicon-on-insulator chip. If this research is successful, the optical circuits, using PbSe quantum dots, would provide a source of non classical light capable of providing single photons on-demand.

Currently used optical circuits incorporate PbSe nanocrystals on the surface of ultra-small optical cavities created in a 200 nm thick silicon layer which are fabricated using high-resolution lithography and dry etching techniques. These devices are designed to maximize the dipole coupling of the electrons in the nanocrystals with the electric field of the fundamental mode supported by the microcavities. The strength of the dipole coupling is limited by the volume of the microcavity, and the dipole transition moment of the electrons at the fundamental resonance of the nanocrystals. In order to enhance this coupling, the sponsors are investigating the incorporation of single crystal metal (Ag or Au) flakes, 10 nm by 50 nm by 50 nm in dimension, in the microcavities to act as local antennae.

However, the sponsors needed to characterize the optical response of the nanoparticles before they can determine the effects of incorporating the nanoparticle in the microcavity. The sponsors wanted a device that is capable of measuring the scattering spectrum of light from individual metal nanoparticles in the visible and near infrared portions of the spectrum.

The sponsors constructed the Nanopositioner apparatus consisting of an optical microscope that focuses a beam of light on to a sample placed on a stage capable of moving in 3 dimensions. A previous student who worked on the project, wrote a LabVIEW program which was used to control the Nanopositioner apparatus. (Y. Clough, 2011) However, the student did not have enough time to implement control of the piezo actuators. This is an essential requirement for the project in order to

move the stage, which utilizes both stepper motors and piezo actuators, to position the stage with sub-micron accuracy in all 3 dimensions. Our primary goal for this project is to enhance the apparatus so that it was capable of performing scans of an area of interest containing the nanoparticles to be analyzed. This involves creating a software routine in LabVIEW that implements a fully-functional control system for the Nanopositioner apparatus. The final system is able to control the stepper motors, in order to align the focused beam of light with the center of a region of interest delineated by circular markers. Then, the apparatus can perform a raster scan the region of interest by using the piezo actuators to move the stage in sub micron increments.

The original project outline is located in Appendix A.

2 Discussion

2.1 Imaging Geometry

There are several ways to perform spectroscopic microscopy. For the purpose of this project, the methods can be broadly classified as coherent or incoherent. Both can be carried out either in reflection or transmission geometries. This project uses coherent scattering, where the detected wavelength is the same as the excitation wavelength, in the forward (transmission) geometry. Florescent (incoherent) imaging relies on detection of radiation at different wavelengths to those used to excite the sample. Fluorescence imaging works well at macroscopic scales, but encounters signal-to-noise ration (SNR) limitations while trying to image single emitters. The SNR ratio of florescence measurements of single emitters is lower compared to coherent forward scattering type imaging of single emitters when the single emitter is weakly excited. (G. Wrigge, 2008) Wrigge et al found that the fluorescence measurements became lost within the noise inherent within the light detector at low light intensities. However, when using transmission methods, it was still observable even with low light intensities.

Our setup was designed primarily for transmission, and could be used either in bright or dark field geometries by placing appropriate apertures in the input and output optical paths. Fiber-coupled input allows for fixed or tunable laser excitation, or white-light excitation of particles in the imaging plane between two high power objectives. The transmitted radiation can be imaged on a camera, directed to a photodetector, or sent to a spectrometer. This apparatus therefore allows for several types of transmission spectroscopic analysis, but all of these options require the incident light from the fiber to be imaged on the sample surface, ideally so that a single metal nanoparticle is excited by the imaged spot.

Apparatus and System

2.1.1 Experimental Setup

Figure 1 shows the Nanopositioner apparatus used to move the glass slide with dilute metal nanoparticles dispersed on its surface, in three dimensions with ~20 nm precision.
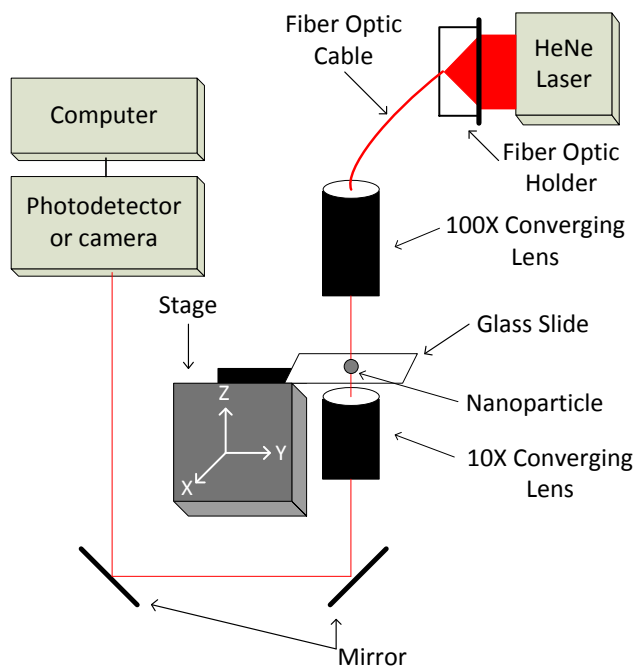
Figure 1: Nanopositioner apparatus diagram

The light source used for the apparatus was a 5 mW HeNe laser (λ = 633 nm). The laser was directed through a lens which focuses the laser beam to a diameter small enough to enter the open end of the single mode fiber optic cable. The end of the cable was held in place by a fiber optic holder assembly. This assembly is shown in Figure 2. The assembly allowed the end of the cable to be precisely positioned in three dimensions. This was important because the beam size of the laser was extremely small, and needed to enter the fiber optic cable, which was about 4 μm in diameter, thus it was necessary for the fiber to be positioned with high precision to ensure that a maximum amount of laser light was directed into the fiber.
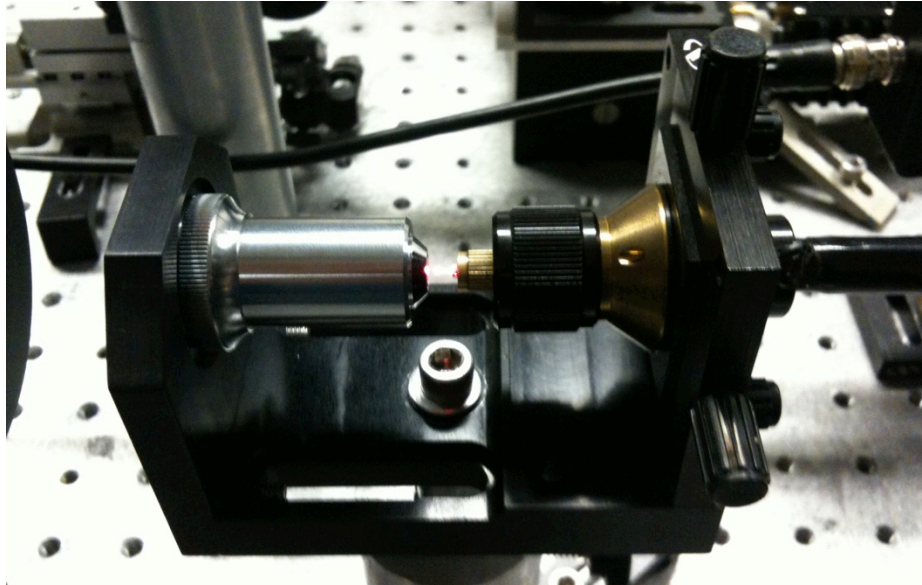
Figure 2: Fiber holder assembly

The fiber optic cable transported the laser light to a 100X objective lens which focused the beam onto the slide containing the nanoparticles to be investigated, to a spot size of ~2µm. The beam then travelled through the slide then was passed through a 10X objective lens. This region of the apparatus is shown in Figure 3. Finally, the beam was redirected with mirrors into a photo detector or a camera. This is shown in Figure 4. The photo detector contained a photo diode that output a voltage with a linear relationship to the intensity of the light incident on the detector for low and moderate intensities. This voltage was then recorded with a National Instruments Data Acquisition System. If the camera is used, its output an image it sent to a monitor, displaying the magnified image of the sample, facilitating positioning the sample.

Figure 3: Slide and converging lens

Figure 4: Mirrors, stage and photo detector

We used the Melles Griot Nanomax TS model stepper motors for moving the stage. They have a movement range of 15mm and a minimum st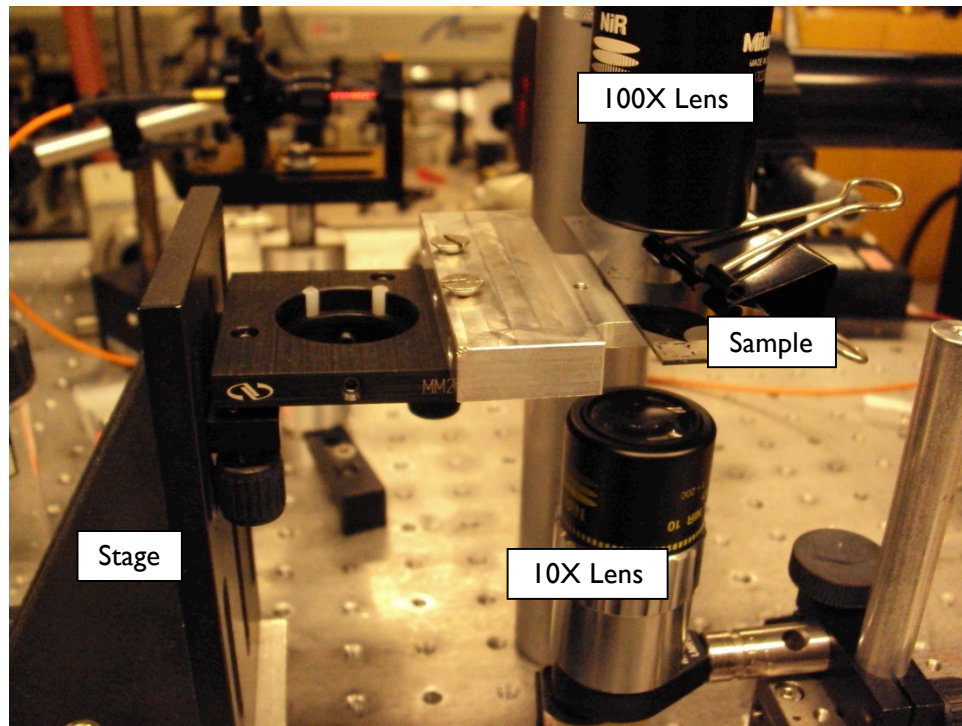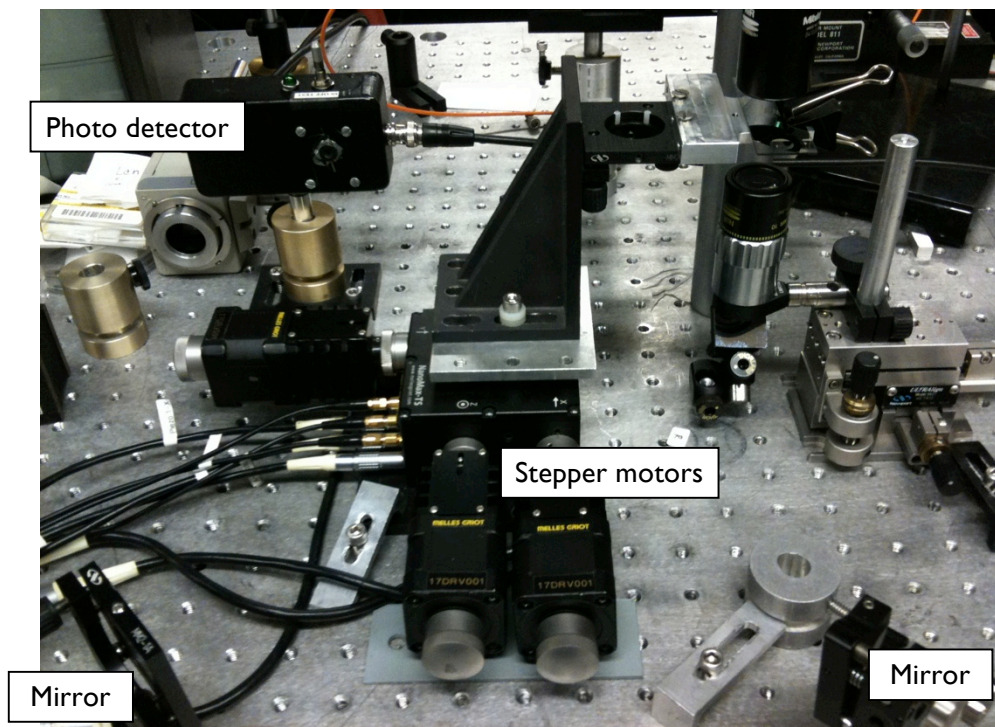ep size of 0.1 μm, according to the datasheet. However, through experimentation it was found that the accuracy of the stepper motors degraded at step sizes less than 1 μm. The stepper motors appeared to step in unequal step sizes when run in this regime. Thus, the minimum usable step size was 1 μm, which still met the requirements of our application. The stepper motors have two methods of control: manual and computer control. Knobs on each of the stepper motors allow the user to position the stepper motors in 1-2 μm increments. The stepper motors were also connected to a computer via the stepper motor controller module allowing us to position the stepper motors using LabVIEW. The motor control module is shown in Figure 5. When using computer control, the motor controller kept track of the position of the stepper motor, allowing the stepper motor to be moved to an arbitrary absolute position. However, the motor controller was not aware of movements caused by using the manual control knobs. This led to limitations when using the manual control knobs and computer control in combination.

Figure 5: Stepper motor and piezo control module

We used the Melles Griot 17DRV001 piezo actuators to scan for the nanoparticles. The piezo actuators utilize the piezoelectric effect to achieve actuation. The piezoelectric effect is a material property in which an applied electric field to the material causes it to expand or contract. Resolutions on the nanometer scale are therefore achievable with the piezo actuators, utilizing this effect. For this particular model, the smallest position increment was 5 nm and the maximum travel range was 20 μm. Just like the stepper motors, the piezo actuators have manual control knobs and computer control. It is highly recommended that the manual control knobs are not used and were always set to their zero position. This is because the LabVIEW drivers appeared to have an error causing the piezo actuators to move to an incorrect position when the knobs' positions are non-zero.

Additional photos of the experimental setup are located in Appendix B.

2.2 Scanning Procedure

Ultimately, the apparatus allows light intensity information to be collected while moving the stage containing the sample with nanometer precision. This was done using LabVIEW to automate this procedure, first to find the center of the alignment markers where the nanoparticles were placed using the AFM, then to record the intensities of the light.

2.3 Nanoparticle sample

In order to determine the position of the single nanoparticle we are performing spectroscopy on, a thin metal pattern of alignment markers was deposited on a glass slide by Mark Greenburg in the lab. The reference markers consist of 6 symmetrically placed segments of width 5 μm, placed along a circle of diameter 100 μm. The reference markers are shown in Figure 6. Then, a 10 μm square region at the center of the markers was swept clean of nanoparticles and a single particle was positioned near the center of the square region. Jonathan Massey-Allard used an atomic force microscope (AFM) to position the single nanoparticles.
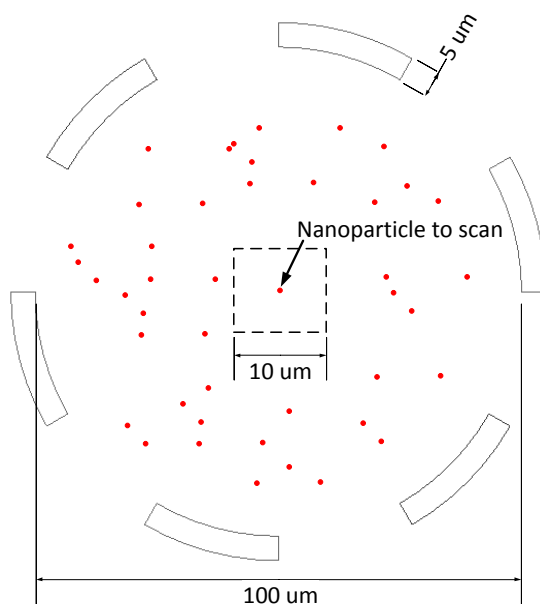
Figure 6: Diagram of alignment markers

Our optical setup and software had to first position the laser beam as close to the center of the reference markers as possible. This was done using stepper motor control. Once at the center, 20x20 μm square raster scans were carried out using the piezo actuators and while scanning, the transmitted signal from the photodetector was recorded. This scanning process was performed at different Z heights, which changes the position of the focal point of the beam relative to the slide. This was necessary because the depth of focus of the imaging system is only on the order of a few microns, and it isn't possible to manually adjust the focus without misaligning the optics. Ideally, when scanning a single nanoparticle, we should see a 20x20 μm blank square region of high intensity with a small region of lower intensity appearing somewhere in the scan region for a few of the images obtained at Z values close to the focal point of the beam.

2.3.1 Center Finding Algorithm

Since it was difficult to determine the center of the reference markers manually, we needed to select an algorithm to automate the center finding. This was one of the requirements of this project made by the sponsors. Automated center finding is necessary for reproducibility of scans, and to avoid touching the apparatus during the data collection process, which could cause misalignment. The stepper motors are used to position the stage during center finding because they have a travel range large enough to cover the entire diameter of the reference markers. We considered three options before choosing one to implement.

2.3.1.1 Option 1

Option 1 was to scan all the reference markers to create an image of the surface. An example of such an image is shown in Figure 7. Some form of image recognition can be used to determine the center of the reference markers. The benefits of this method are that it would be extremely accurate. However, the downsides are that it takes a very long time to scan the entire surface (~1 hour) and we would need a MATLAB license on the computer to use MATLAB to implement an image recognition algorithm.
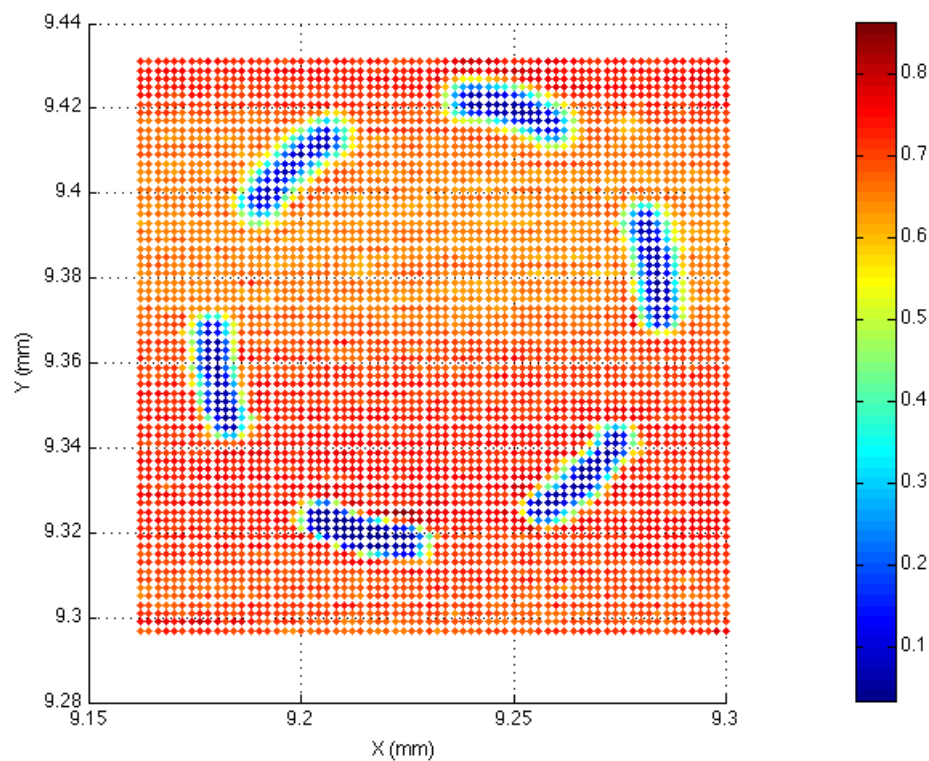

Figure 7: Image of all markers

2.3.1.2 Option 2

Option 2 was to first perform a scan in the x direction and look for two markers. The center point between the markers corresponds to the center of the markers in the x direction. The same procedure is then repeated in the y direction. This process is shown in frame 1 of Figure 8.
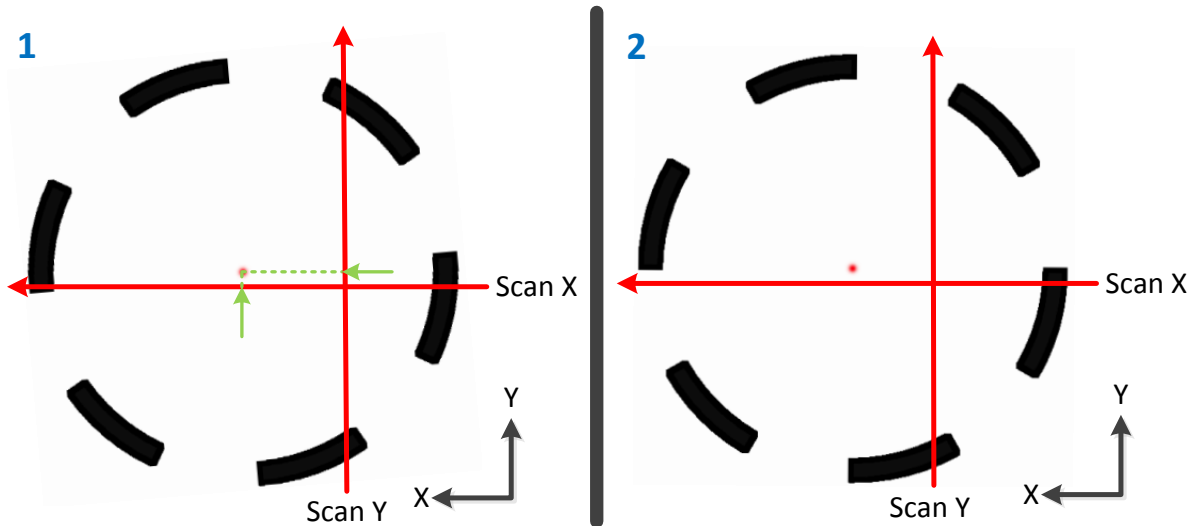
Figure 8: Centre finding algorithm option 2

The benefits of this algorithm are that it can be very fast, since at minimum, only one row and one column need to be scanned. The downside is that the algorithm wouldn't work for an arbitrary rotation of the markers. This is shown in frame 2 of Figure 8, where only one marker segment is detected for each row / column scan.

2.3.1.3 Option 3

The idea behind of option 3 is to scan in order to find the boundaries of the reference markers. A diagram showing the center finding procedure is shown in Figure 9, and is broken down into 6 steps. Before the procedure begins, the beam must be positioned to the right and below the markers.

Figure 9: Centre finding algorithm option 3

The algorithm used for option 3 is described below. Pseudocode for these steps is located in Appendix C.

Step 1

The procedure begins scanning rows by moving the stage in the positive x direction. If the reference markers are not encountere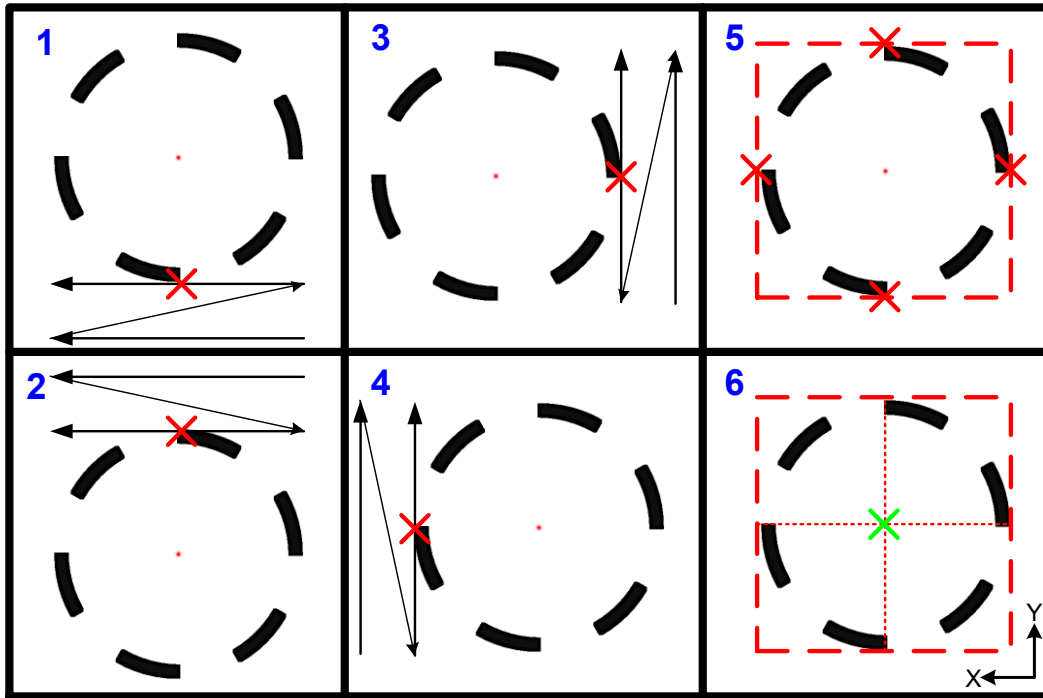d during a row scan, the stage is moved one increment in the positive y direction. This is shown pictorially in frame 1 of Figure 9. If the photo detector voltage drops below a configurable threshold voltage for three successive steps then the algorithm considers the edge of a marker to have been found. Three successive steps are used in order to ensure that the object is a marker, and not small dust particles or random signal fluctuation. Once the edge of a marker is found, the y distance at which the edge was found is recorded.

Step 2

The stage is then moved in the positive y direction until the beam is positioned above and to the right of the markers. Then, rows are scanned, in similar fashion to step 1, except that the stage is moved in the negative y direction after the scan of each row is completed. Once again, the y position at which the marker is encountered is recorded.

Step 3

The stage is moved to the starting position of the scan. Then, columns are scanned by moving the stage in the positive y direction. If the marker is not detected while scanning a column, then the stage is

moved in the positive x direction. This process repeats until a marker is detected and the corresponding x position of the stage is recorded.

Step 4

The stage is moved to the bottom left extent of the scan area. Then, similarly to step 3, columns are scanned by moving the stage in the positive y direction. This time, the stage is moved in the negative x direction after scanning a column. Once a marker is detected, the x position is recorded.

Step 5

Now we have four data points which define a bounding box that encompasses the reference markers. This is shown in frame 5 of Figure 9.

Step 6

The center of the bounding box, which is easy to calculate, corresponds to the center of the reference markers. The stage then moved to the center of the markers.

The benefits of this algorithm are that it is versatile, in that it could find the center for any symmetric pattern of alignment markers. It also can be relatively fast. The downside is that the user needs to guess how big to make the scan area before beginning the scan. If the scan area is too small, the user won't know because the algorithm will complete, but won't provide any indication that it didn't move to the center of the markers. In option 1, the user still needs to select a scan area, but once the scan is complete, the image of the markers can be displayed which can tell the user if the scan area was too small.

The following table summarizes all three options.

	Speed	Accuracy	Complexity	Versatility
Option 1	Slow	Very high	High	Good, but need to change image recognition algorithm for different shapes.
Option 2	Fast	Can fail depending on orientation.	Low	If a closed shape is used it can be versatile.
Option 3	Medium	Good	Medium	Works for symmetrical shapes.

We decided to use option 3 because it met our requirements and has balanced performance parameters. Before implementing the algorithm in LabVIEW, we first simulated the results by running the algorithm on the image of all the markers in Figure 7. The result is shown in Figure 10 where the centre point found by the algorithm is the blue dot in the centre of the image. The MATLAB code used to perform the simulation is shown in Appendix E. From the simulation results, we concluded that we could proceed with implementing the algorithm in LabVIEW (See Appendix D).
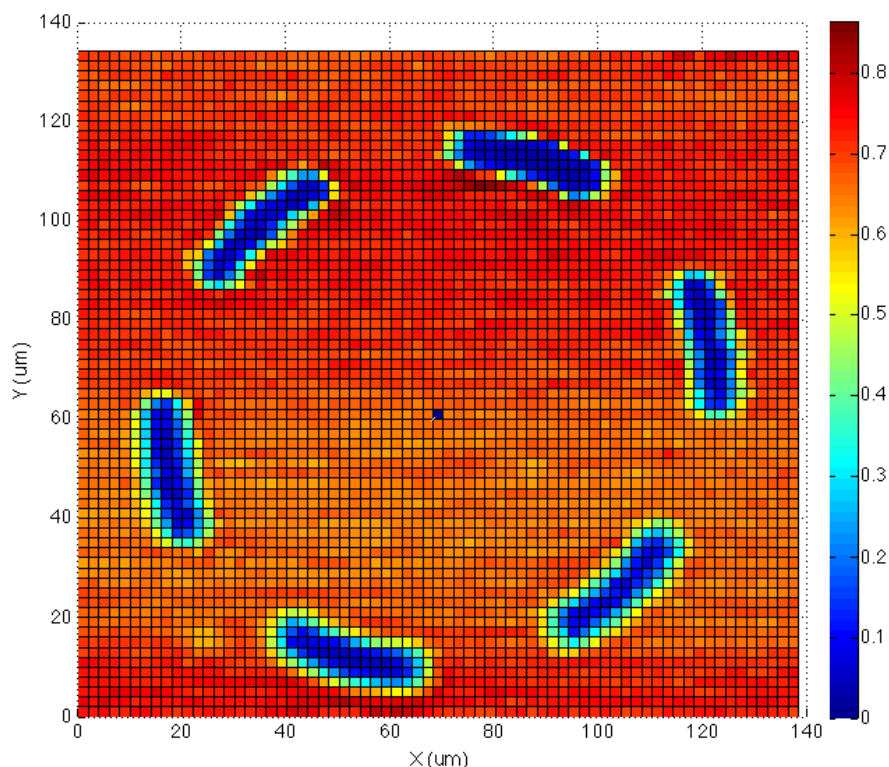

Figure 10: Centre finding algorithm simulation results

In order to set up the apparatus so a scan could be performed stage was manually positioned with stepper motors so that the focused laser was located to the bottom right of the alignment markers. This

was performed by first, installing the camera. Then, the top objective was defocused so that the surface features were discernable. Then manual stepper motor positioning was used to move the stage until the alignment markers were visible on the camera output. The top objective was then focused so that the spot size on the camera was as small as possible. Finally, the stage was moved so that the beam was positioned to the bottom right of the alignment markers as seen on the camera output. This is shown graphically in Figure 11.
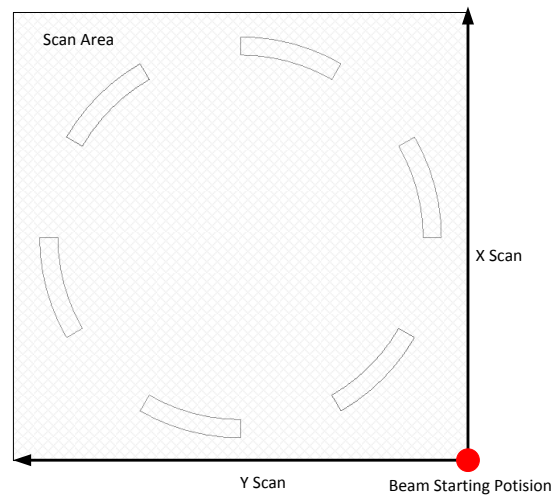

Figure 11: Centre finding algorithm setup

The pseudocode for the center finding algorithm is available in Appendix C, as are images of the entire LabVIEW implementation, located in Appendix D.

2.3.2 Particle Scanning

Piezo actuators were chosen for this application, as they have 5nm position increments. In contrast, the stepper motors have a minimum 1μm step size, and demonstrated excessive vibrations when in motion. This was not ideal for the raster scan recording the intensities of the light, as the signal was sensitive to the vibrations.

After the beam was located at the center of the alignment markers, the piezo actuators were used to offset the sample from the center. The amount of offset was based on the user-specified scanning dimensions, as is shown in Appendix D.

Next, the piezo actuators were used to performed a raster scan by moving the stage in user-specified increments, in both x and y directions. The intensities of the beam were recorded over the entire specified area.

When aligning the sample in the z-direction, it was difficult to position the top surface of the slide at the exact focal point of the beam. The alignment markers were used as a reference to determine when the image was focused, but the markers have a height on the order of a micron which means the beam may

be focused on the top of the markers and not on the surface where the nanoparticles are located. Therefore, as the focal plane was difficult to locate precisely using this method, the piezo actuators included a capability to perform raster scans in multiple z positions.

The particle scanning was automated with LabVIEW as well, and an overall GUI which integrated the stepper motor center finding algorithm, and the piezo actuator raster scanning, was created for experimentation. These LabVIEW panels are located in Appendix D.

2.4 Testing

2.4.1 Background
Several methods were used to verify that the LabVIEW control software was working correctly.

The first step we took was to use the LabVIEW program written by the previous student who worked on the project, and verify that the stepper motor positioning was working correctly. We scanned single segments of the reference marker, and produced images like the one shown in Figure 11. We looked at characteristics such as the width of the marker and its length, comparing them to the actual values. We found that originally, the distance measurements we incorrect by a factor of 2, due to incorrect stepper motor configuration settings. We implemented a software workaround to fix the scaling issue.
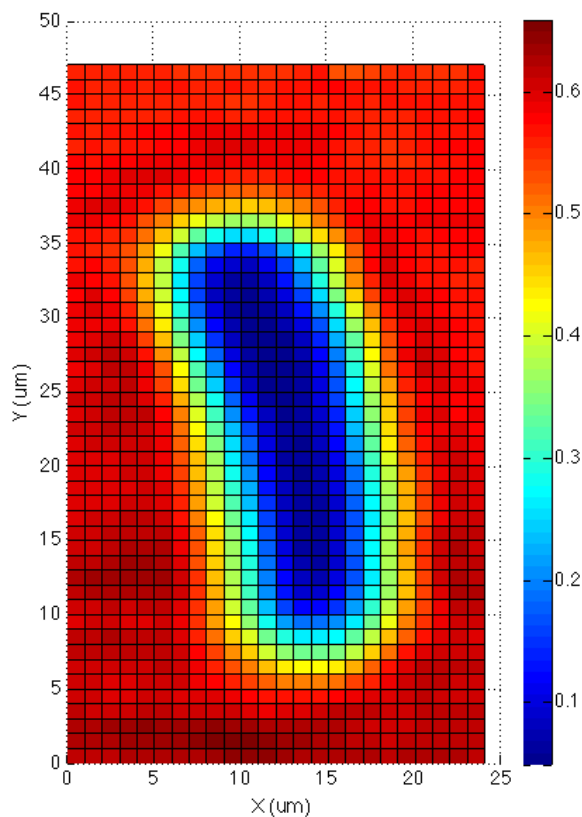

Figure 12: Stepper motor scan of reference marker

Next, we verified that the piezo scanning software routine was working correctly by testing it with two different methods. The first method used was to view the image of the surface, using the camera, while the piezo actuators were scanning the surface. This allowed us to visually see the movement of the stage in real time. The second method used to verify the correctness of the piezo actuators was to scan reference objects on the surface while collecting the light intensity measurements using the photo detector. The images obtained from the intensity measurements were compared to the camera images to verify that the piezo scan produced accurate images.

In order to verify the center finding algorithm, we first of all, executed the center finding algorithm and simulated the photodetector output within LabVIEW by controlling the intensity with a button on the program's GUI while looking at the image of the surface on the camera output. This approach allowed us to watch, in real time, the movement of the stage on the screen as the various steps of the algorithm were executing. We could then verify that the algorithm was working correctly by ensuring the proper actions were taken for each input. The next step was to run the algorithm on the reference markers, using the photodetector output as an input to the program. The ideal way to verify that the algorithm was working correctly was to locate the center, and then proceed to perform a piezo scan of an easily detectable reference object placed in the center of the markers. Unfortunately, we were not able to place a suitable reference object in the center. As a result, we verified the algorithm by allowing it to locate the center, then replacing the photodetector with the camera without moving the stage. We then could see the center point that the algorithm found and check to see if it was in the center of the reference markers. We found that the algorithm was able to locate the center to within about a 5 μm, which is adequate for this application.

2.5 Results

In this section we will present the data that we obtained using the Nanopositioner apparatus.

We first scanned a sample containing a group of nanoparticles < 1 μm in diameter as shown in the AFM image of the sample in Figure 13. The nanoparticles were positioned in the center of the reference markers using the AFM. We then scanned the center of the reference markers using the Nanopositioner and obtained the images shown in Figure 14 (MATLAB code for creating these images is in Appendix E). Since the spot size of the beam is 1 μm in diameter, we can only resolve objects which are larger than 2 μm. Objects that are smaller will still appear to be 2 μm. Thus, when we image the sub micron nanoparticle collection, they appear to be about 2 μm in diameter. Comparing the two images, there seems to be a correlation between the positioning of the individual nanoparticles in the AFM image and the regions of high intensity in the Nanopositioner data. The nanoparticles at x = 8 μm and y = 4 μm in Figure 13 correspond to the high intensity region at x = 6 μm and y = 5.5 μm in Figure 14. Also, the two nanoparticles which are below the aforementioned nanoparticle collection are visible in Figure 14 below the larger region of high intensity This suggests that the data from the Nanopositioner is in fact the nanoparticles and not some other object on the surface.
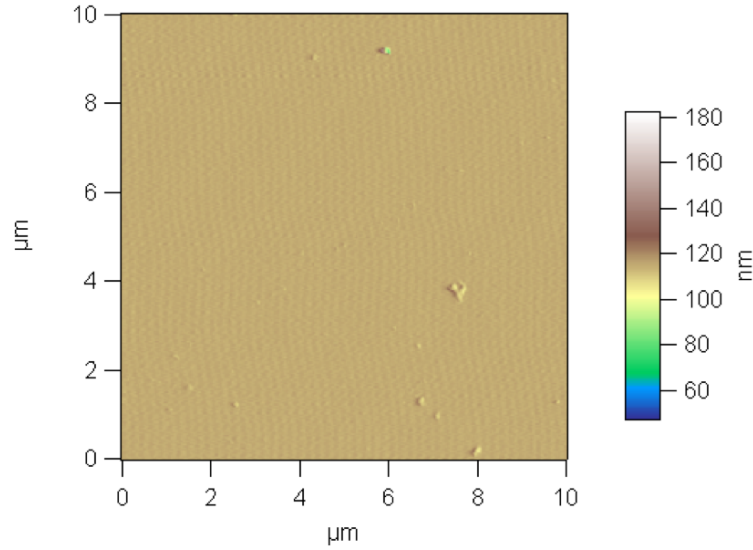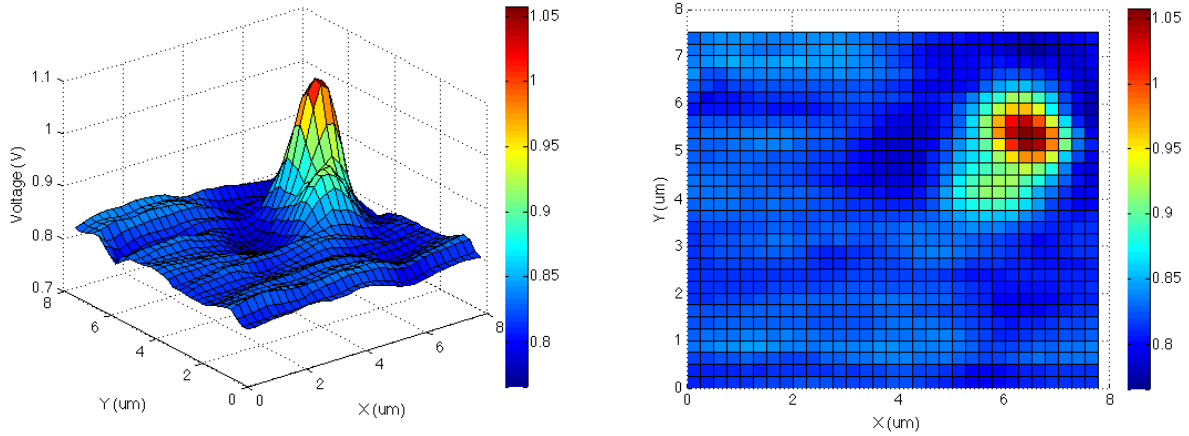
Figure 13: AFM image of nanoparticle collection

Figure 14: Nanopositioner image of nanoparticle collection

We can examine both the contrast and the signal-to-noise ratio of the data to quantify the scan results. First of all, contrast C is defined as $C = \frac{Peak\ intensity - Background\ intensity}{Background\ intensity}$. The signal-to-noise ratio is defined as $SNR = \frac{Peak\ intensity - Minimum\ intensity}{RMS\ noise\ amplitude}$. The RMS noise amplitude is calculated by taking a sample of noise from the data, computing its mean, then subtracting the mean from the data points. This centers the noise about 0. Then, the RMS amplitude is calculated by squaring each zero- centered data point, computing the mean, then taking the square root.

For this scan we calculated C = 0.2864 and the SNR = 24.39. Also, the RMS noise was calculated to be ± 0.0142 V

We then scanned a different nanoparticle sample shown in Figure 15. The scan was performed with a different fiber holder assembly than the one used for the data above. This sample has a relatively clear area surrounded on two sides by a line of nanoparticles. The scan from the Nanopositioner is shown in Figure 16 and Figure 17.
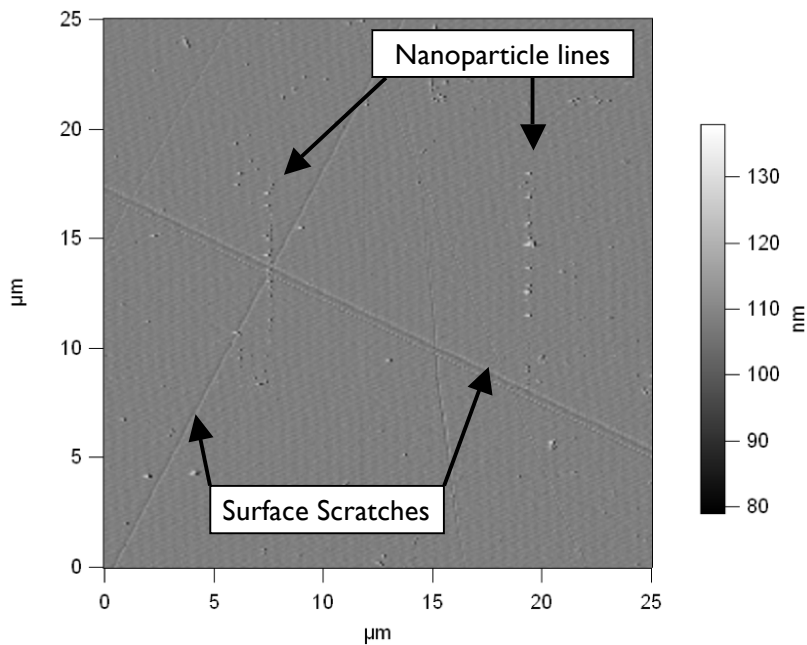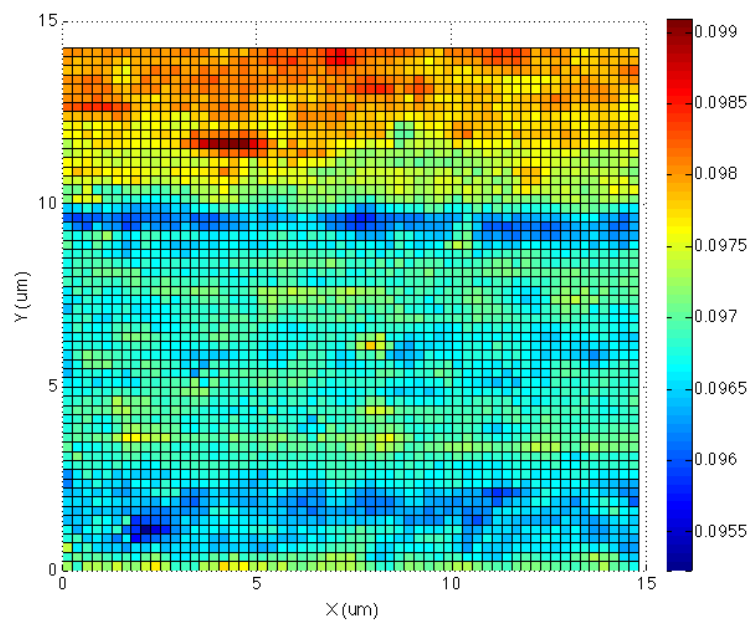

Figure 15: Nanoparticle line AFM image

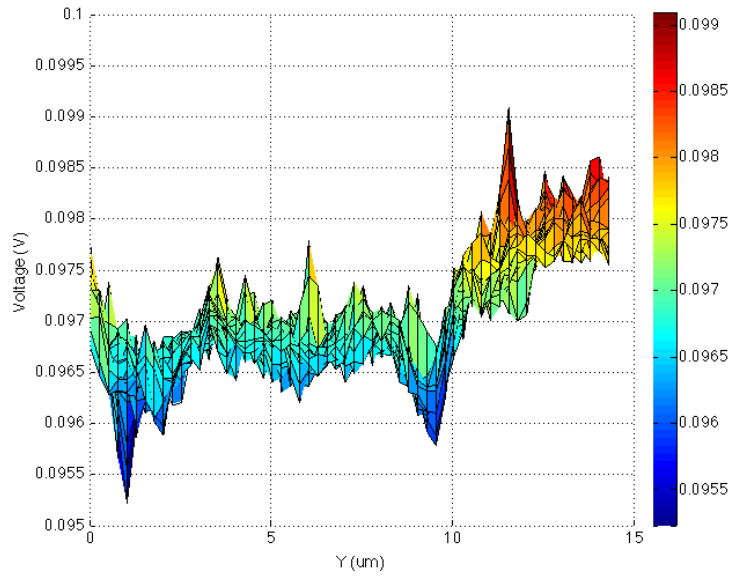Figure 16: Nanoparticle line scan top view

Figure 17: Nanoparticle line scan side view

We calculated that the RMS noise was ±0.000276 V with an average background voltage of 0.0966 V. The amount of noise in the data is much lower with the new fiber holder assembly that was used to take this image. For the scan in Figure 14, the RMS noise was ±0.0142 V with an average background level of 0.82 V. With the new fiber holder, the amount of noise has been significantly reduced.

In Figure 17 the average intensity is slowly varying as y increases. However, the signal is punctuated by a few sub micron wide spikes. We believe that this is noise on a slowly varying striped background which may be due to swabbing the glass slide when it was cleaned.

We took another set of scans after translating the stage in the y direction by about 6 μm. The data is shown in Figure 18 and Figure 19.
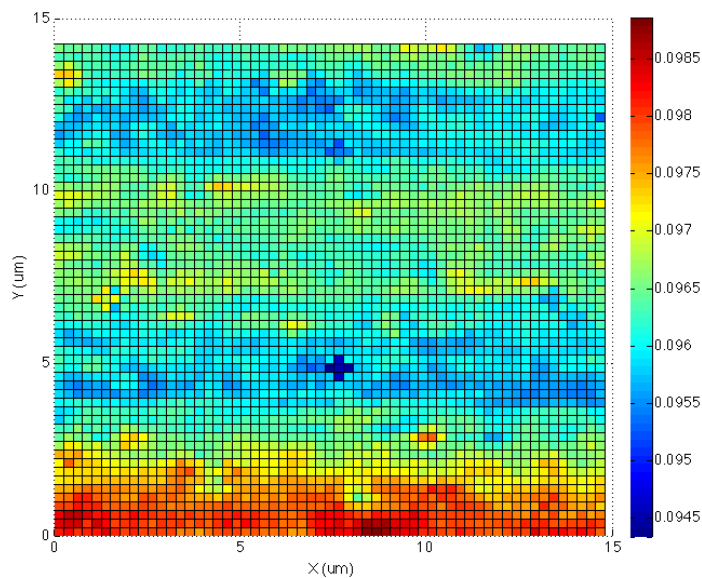
Figure 18: Nanoparticle line scan 6 μm Y translation top view
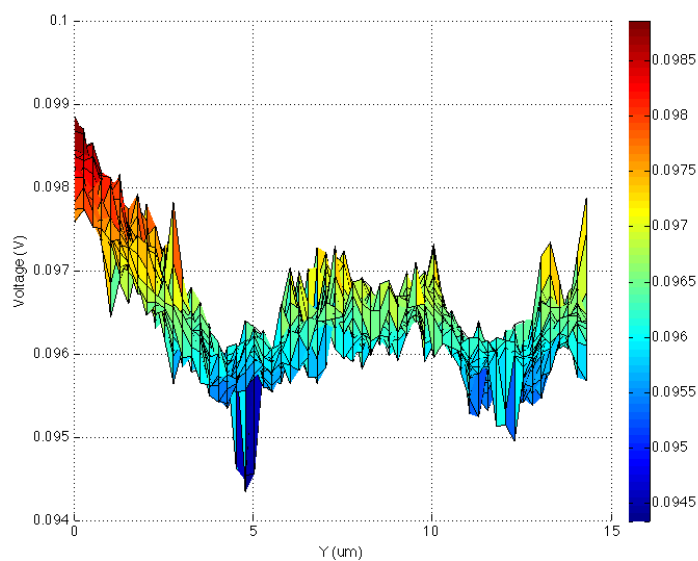

Figure 19: Nanoparticle line scan 6 μm Y translation side view

From both sets of data, we can see that bands of high and low intensity were detected once again. However, it is not possible to determine if the bands are caused by the lines of nanoparticles, or are caused by low frequency noise in the signal. We can see from both sets of data that there appears to be

some irregular features such as the region of high intensity at x = 4.5 μm, y = 13 μm in Figure 16, as well as the region of low intensity at x = 7.5 μm, y = 5 μm in Figure 18. However, since the features are < 2 μm, the features are just noise.

Next, we scanned residue on the surface of the glass slide in order to characterize the contrast of the data taken from the apparatus. We performed the scan at various Z heights in order to obtain images with the sample at different positions near the beam's focus. The results are shown in Figure 20.
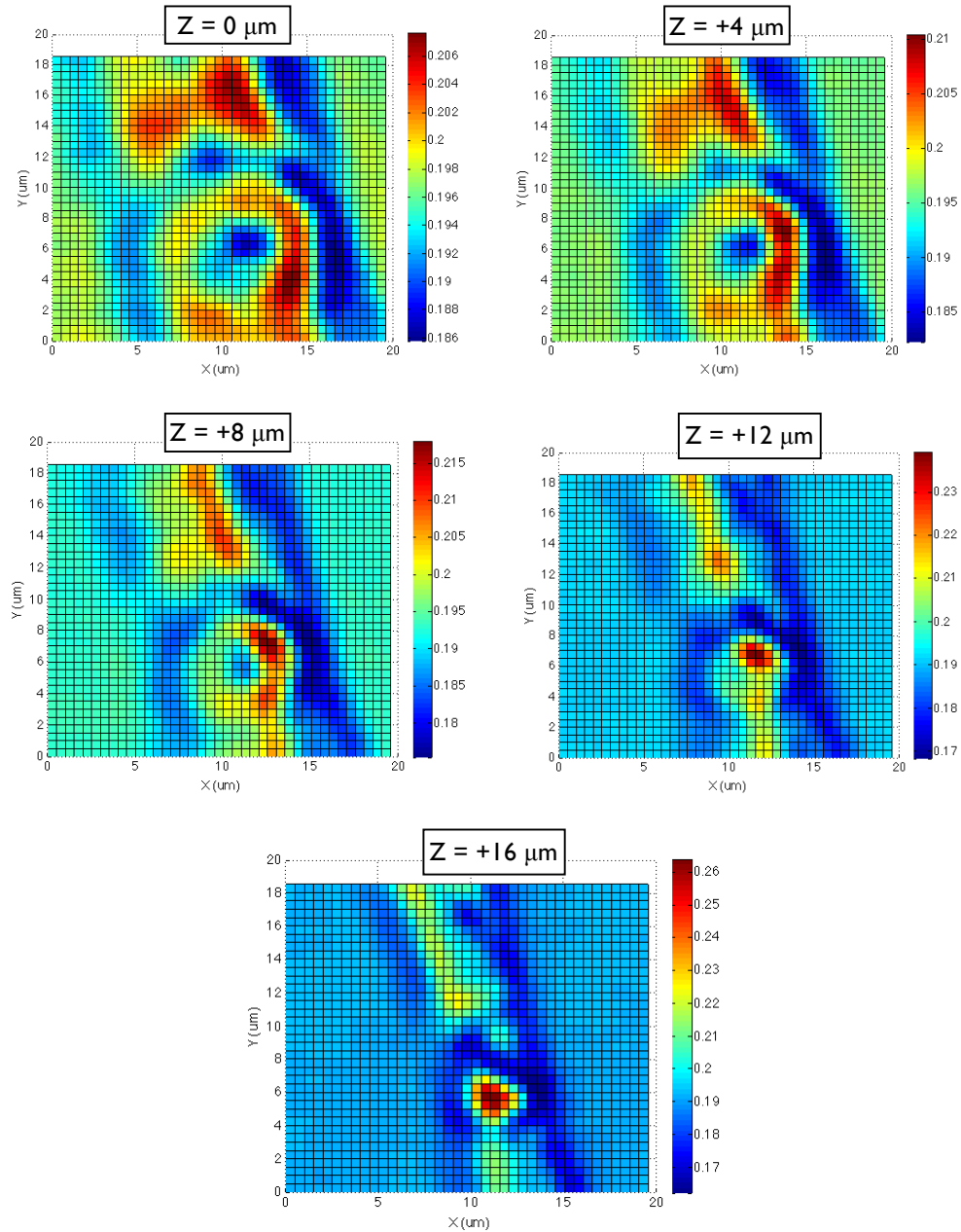

Figure 20: Scan of residue at various Z levels

It is evident from the images that the object being image become focused as the Z height is increased. Another observation about this data is that, even though we are performing transmission imaging, the object being imaged appears as an intensity enhancement rather than an intensity drop. This is likely caused by the numerical aperture of the bottom objective lens being smaller than the numerical aperture of the top lens. This can cause a diffraction pattern to be formed that shows the object as an enhancement rather than an intensity drop. We verified this by performing another scan of the same spot at a different Z height, and the data displays the object as an intensity drop instead of an enhancement. This scan is shown in Figure 21.
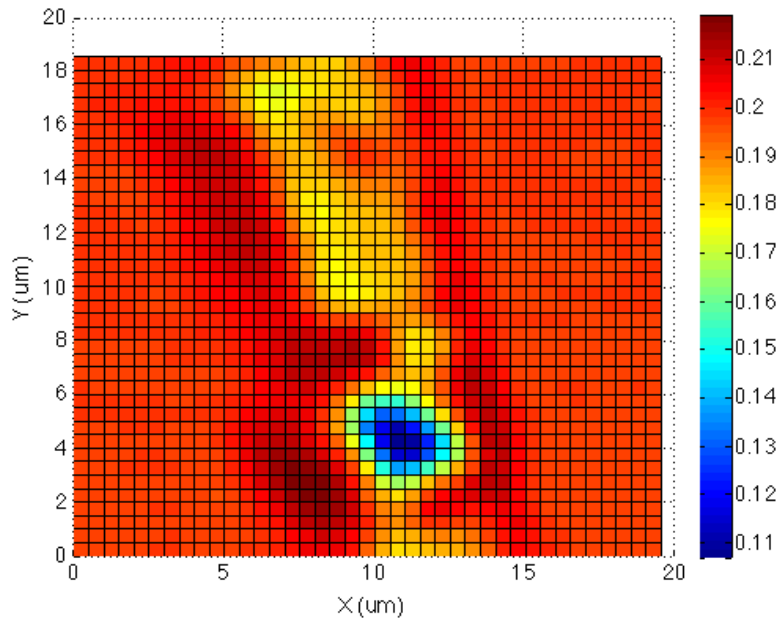
Figure 21: Scan of residue with intensity drop

The scans in Figure 20 show that putting the object precisely in the beam's focus is necessary in order to obtain an accurate image of the surface. Since it is not possible to determine the best Z height proper to performing a scan, the ability to perform multiple scans at various Z heights is absolutely necessary in order to select the image having the best contrast and focus. The image at Z = 16 μm has the smallest resolvable features and also appears similar to the residue we observed on the camera output. For the image taken at Z = 16 μm, we calculated the contrast, C = 0.429, the RMS noise = ±0.000595 V and the SNR = 197, which indicates that this method of performing multiple Z level scans produces higher quality images compared to, for example, Figure 14.

3   Conclusions

The objective of this project was to implement an automated system capable of locating nanoparticles by recording the intensities of laser light passing through the sample. The measurement sensitivity and signal to noise ratio was a key factor in the system performance.

The overall system used to locate nanoparticles implemented a large array of alignment markers, which were used to locate the center where the nanoparticles were approximately located. This central area was then scanned to map the intensities of light from a HeNe laser. Drops in recorded light intensity were used to determine the locations of the nanoparticles. This system was designed and implemented using a combination of stepper motor and piezo actuators, automated with LabVIEW.

The intensity scan taken appeared to resemble the locations of the nanoparticles placed by the AFM, with the bands of intensities. The contrast and signal to noise ratio were shown to correlate to the quality of the data. Further recommendations for improving the SNR and the nanoparticles scans, are addressed in the next section.

4 Project Deliverables

The following table lists the deliverables that will be transferred to the project sponsors. No financial section was included, as all apparatus and software were already present at the beginning of the project.

Table 2: Project Deliverables

Deliverable	Status	Additional Notes	Hand-over Medium
LabVIEW automated code (center finder and scanning mechanism)	Completed	GUI is included	Electronic
Assembly capable of characterizing nanoparticles	Working		In-lab
LabVIEW User manual	In Progress		Electronic
MATLAB scripts for processing data	Completed		Electronic

5 Recommendations

1. The setup was only capable of focusing the light to a minimum spot size of about 2μm, which limits the minimum size of object that can be resolved. A glass hemispherical lens with a refractive index of 2.35 has been purchased The hemisphere will be used in addition to the high power microscope objective as a solid immersion lens with the nanoparticles placed at the bottom of the flat surface of the hemisphere. Using the hemisphere, a smaller spot size could be achieved, which could allow the apparatus to more easily resolve nanoparticles. This was discussed in the original proposal, but was not tested, although the hemisphere is ready for testing.

2. The stepper motors and piezos caused a significant amount of vibrations when moving. The vibrations caused detectable noise in the voltage signal from the photodetector. Reducing the vibrations could decrease the SNR allowing the apparatus to resolve smaller objects. We recommend investigating how the stage is currently secured to see if the vibrations can be reduced.

3. In the current set up, the photo detector and camera are located near the fiber optic holder assembly. When switching the photo detector and the camera, it is necessary to be extremely careful because it is possible to bump the fiber holder with your hand or one of the cables connecting the camera. Since the fiber holder is very sensitive, a bump would cause it to become misaligned. Moving the setup so that the detector would be further away from the cable, or replacing the cable to be more robust, would guarantee reproducibility of intensities between experiments.

4. Increase the signal to noise ratio. Extraneous occurrences such as motion of the fiber optic cable, the sample location in the focal plane, resulted in lower reproducibility and quality of images. Removing these factors could improve the quality of the data.

Appendix A Original Project Proposal

The following is the original project proposal, as posted on the Engineering Physics 459 course page.

"In one of our ongoing research projects, our group needs to be able to detect and measure the optical absorption and emission from single semiconductor quantum dots and nanometer sized metallic particles. One of the difficulties is finding the location of these small structures - that are only ~ 5 – 50 nm in size - with high precision.

Our lab has a nanopositioning system consisting of a high-precision translation stage and a combination of stepper motors and piezoelectric actuators with a resolution of 100 nm and 10 nm, respectively. The system is controlled by a Lab View code that is currently able to control the stepper motors but lacks the control of the piezo actuators. It would be valuable for our project if the piezo actuators could be controlled by the same Lab View routine.   This system is already integrated with high numerical aperture lenses for high-resolution spectral imaging.

The two main tasks of the co-op student would be a) writing the Lab View code, b) testing the precision and reliability of the nanopositioning system, and c) obtaining extinction spectra from metal nanoparticles using the full system."
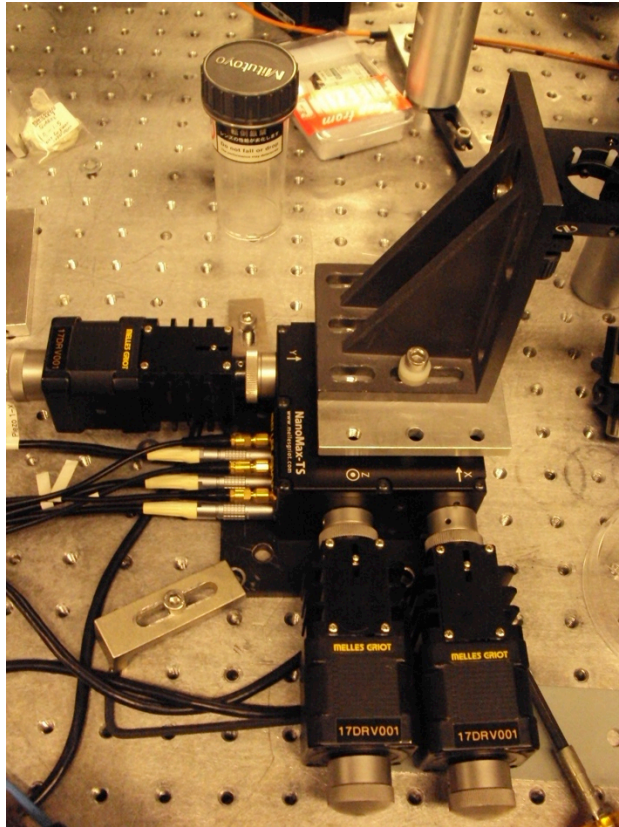
Appendix B Pictures of Experimental Setup

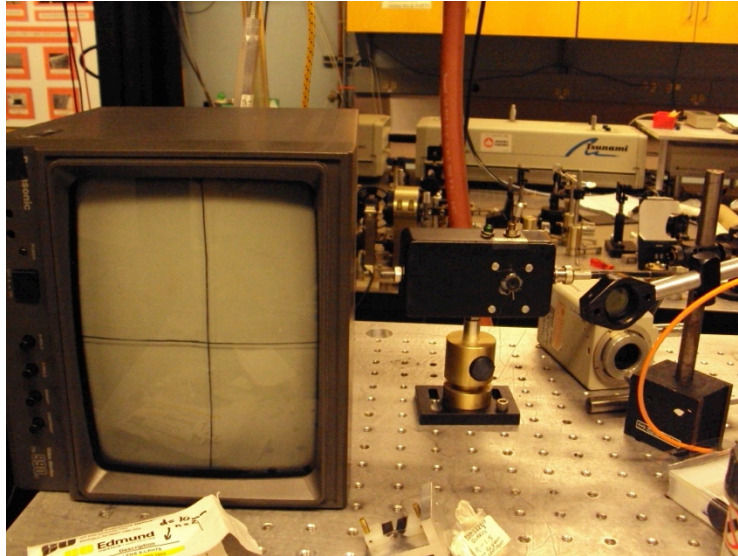**Figure 22: Stage with stepper motors and piezo actuators**

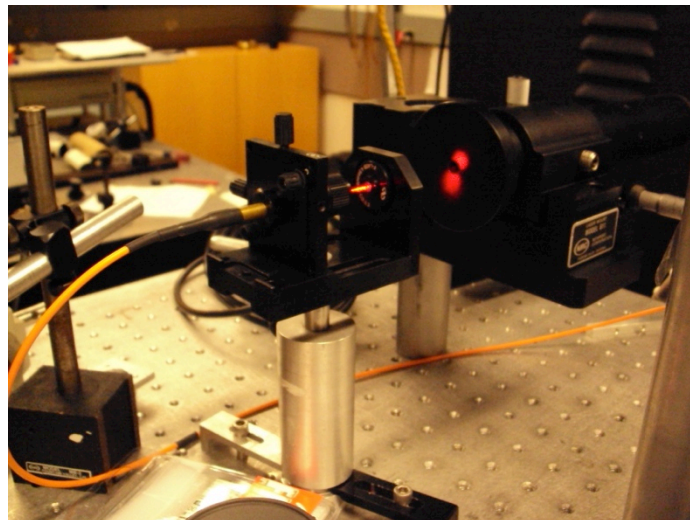**Figure 23: Photodetector and screen close-up**

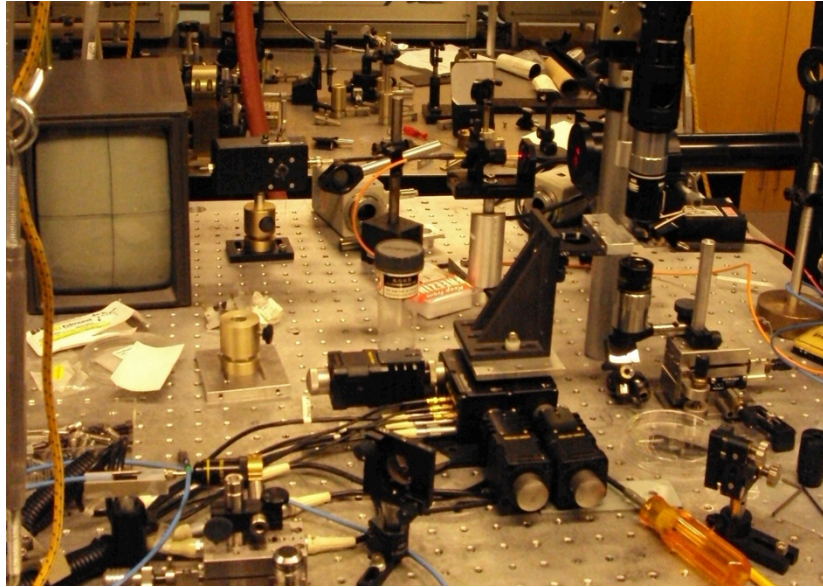**Figure 24: HeNe laser and fiber optic cable**

Figure 25: Entire optic setup

Appendix C Centre Finding Pseudo Code

Below is pseudo code describing how the algorithm is executed. This pseudo code is implemented in the LabVIEW program.

```
// Stage 1

FOR y = 0 to number_of_y_steps
    FOR x = 0 to number_of_x_steps
        SET intensity = Read photodetector voltage
        IF intensity < threshold AND sequence == 0
            SET sequence = 1
        ELSEIF intensity < threshold AND sequence == 1
            SET sequence = 2
        ELSEIF intensity < threshold AND sequence == 2
            SET sequence = 0
            SET saved_x_index = x
            SET saved_y_index = y
            SET position_y1 = Current Y position
            Break out of both for loops
        ELSE
            SET sequence = 0
        END IF
        Move by x_step_size in positive X direction
    END FOR

    Move by y_step_size in positive Y direction
    Move by x_step_size*(number_of_x_steps+1) in negative X direction

END FOR

Move by (number_of_y_steps-saved_y_index)*y_step_size in positive y direction
Move by (saved_x_index+1)*x_step_size in negative x direction

// Stage 2

FOR y = 0 to number_of_y_steps
    FOR x = 0 to number_of_x_steps
        SET intensity = Read photodetector voltage
        IF intensity < threshold AND sequence == 0
            SET sequence = 1
        ELSEIF intensity < threshold AND sequence == 1
            SET sequence = 2
        ELSEIF intensity < threshold AND sequence == 2
            SET sequence = 0
            SET saved_x_index = x
            SET saved_y_index = y
            SET position_y2 = Current Y position
            Break out of both for loops
        ELSE
            SET sequence = 0
        END IF
        Move by x_step_size in positive X direction
    END FOR

    Move by y_step_size in negative Y direction
    Move by x_step_size*(number_of_x_steps+1) in negative X direction

END FOR

Move by (number_of_y_steps-saved_y_index)*y_step_size in negative y direction
Move by (saved_x_index+1)*x_step_size in negative x direction
```

```
// Stage 3

FOR x = 0 to number_of_x_steps
    FOR y = 0 to number_of_y_steps
        SET intensity = Read photodetector voltage
        IF intensity < threshold AND sequence == 0
            SET sequence = 1
        ELSEIF intensity < threshold AND sequence == 1
            SET sequence = 2
        ELSEIF intensity < threshold AND sequence == 2
            SET sequence = 0
            SET saved_x_index = x
            SET saved_y_index = y
            SET position_x1 = Current X position
            Break out of both for loops
        ELSE
            SET sequence = 0
        END IF
        Move by y_step_size in positive Y direction
    END FOR

    Move by x_step_size in positive X direction
    Move by y_step_size*(number_of_y_steps+1) in negative Y direction

END FOR

Move by (number_of_x_steps-saved_x_index)*x_step_size in positive x direction
Move by (saved_y_index+1)*y_step_size in negative y direction

// Stage 4

FOR x = 0 to number_of_x_steps
    FOR y = 0 to number_of_y_steps
        SET intensity = Read photodetector voltage
        IF intensity < threshold AND sequence == 0
            SET sequence = 1
        ELSEIF intensity < threshold AND sequence == 1
            SET sequence = 2
        ELSEIF intensity < threshold AND sequence == 2
            SET sequence = 0
            SET saved_x_index = x
            SET saved_y_index = y
            SET position_x2 = Current X position
            Break out of both for loops
        ELSE
            SET sequence = 0
        END IF
        Move by y_step_size in positive Y direction
    END FOR

    Move by x_step_size in negative X direction
    Move by y_step_size*(number_of_y_steps+1) in negative Y direction

END FOR

// Stage 5 and 6

Move to absolute position (position_x2-position_x1)/2 in X direction
Move to absolute position (position_y2-position_y1)/2 in Y direction
```

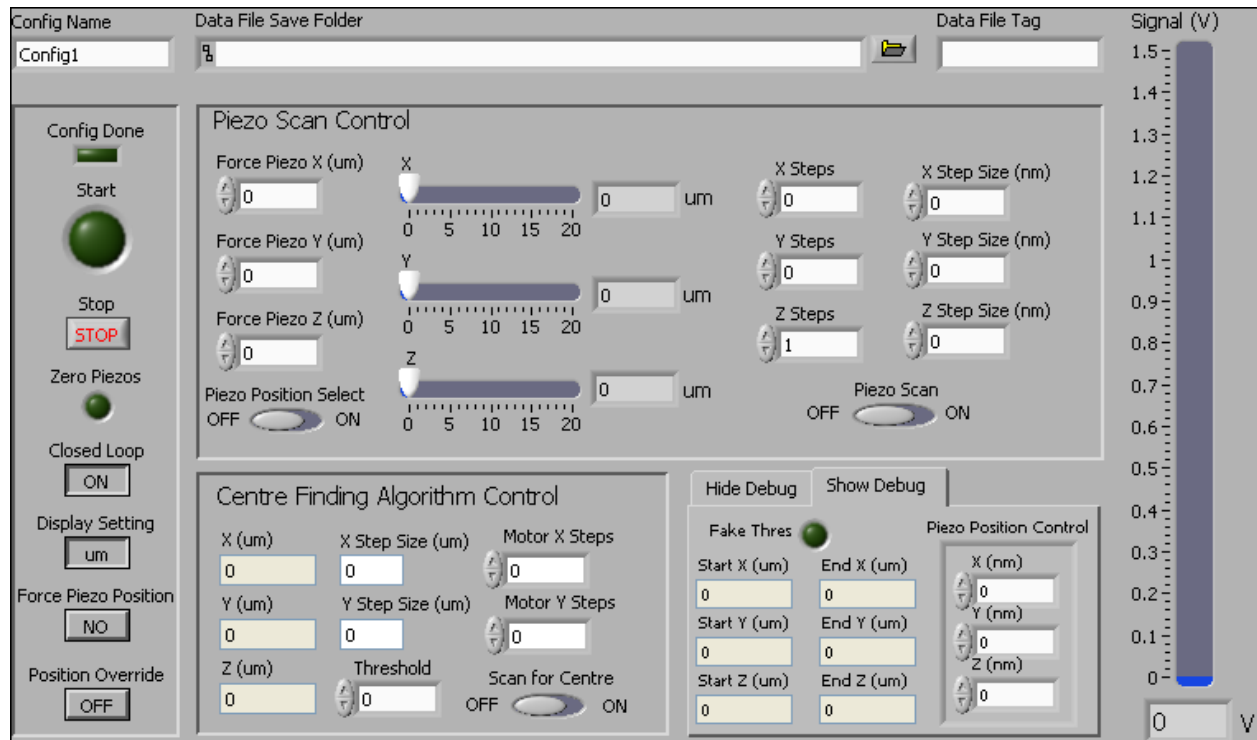# Appendix D LabVIEW Screenshots

Front Panel User GUI

Figure 26: LabVIEW front panel

LabVIEW Code

The following images are the LabVIEW code, in sequence from the beginning of an entire run (center finding algorithm and piezo scanning algorithm). Only the primary code blocks were included.
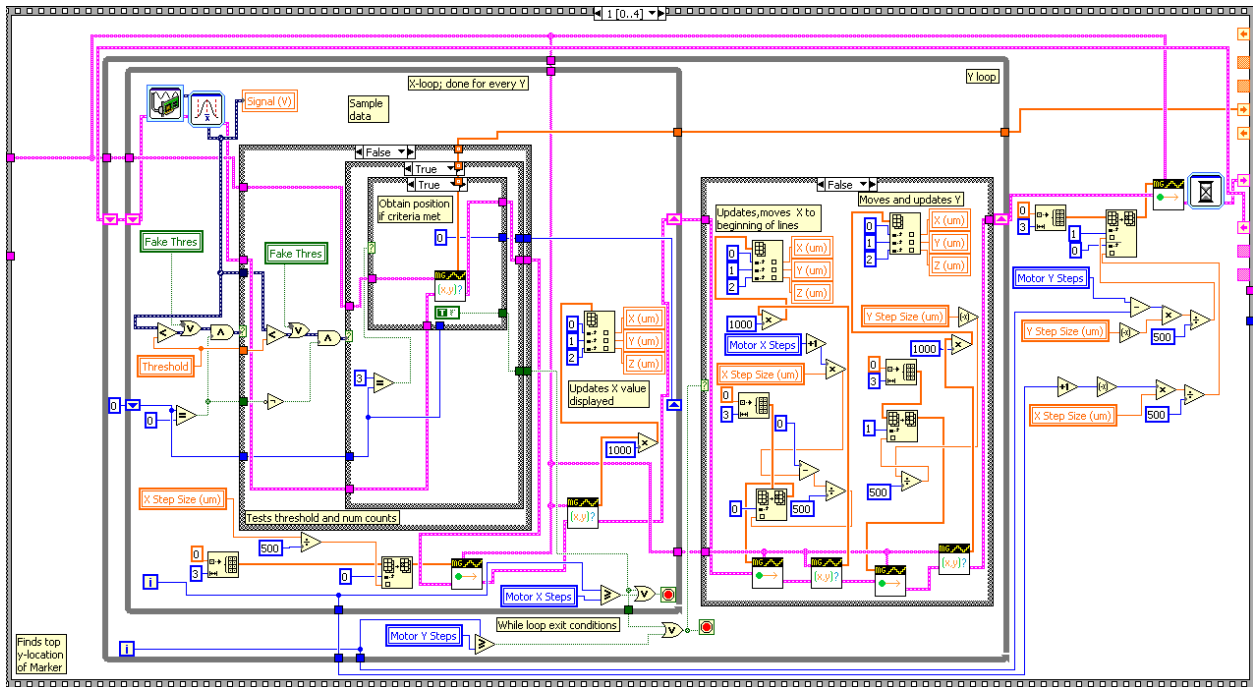

Figure 27: Perform setup for stepper motors and piezo actuators

Figure 28: Option 3 - Center finding algorithm stage 1 of 4

Note that stages 2, 3 and 4 are not shown, but are very similar to stage 1.
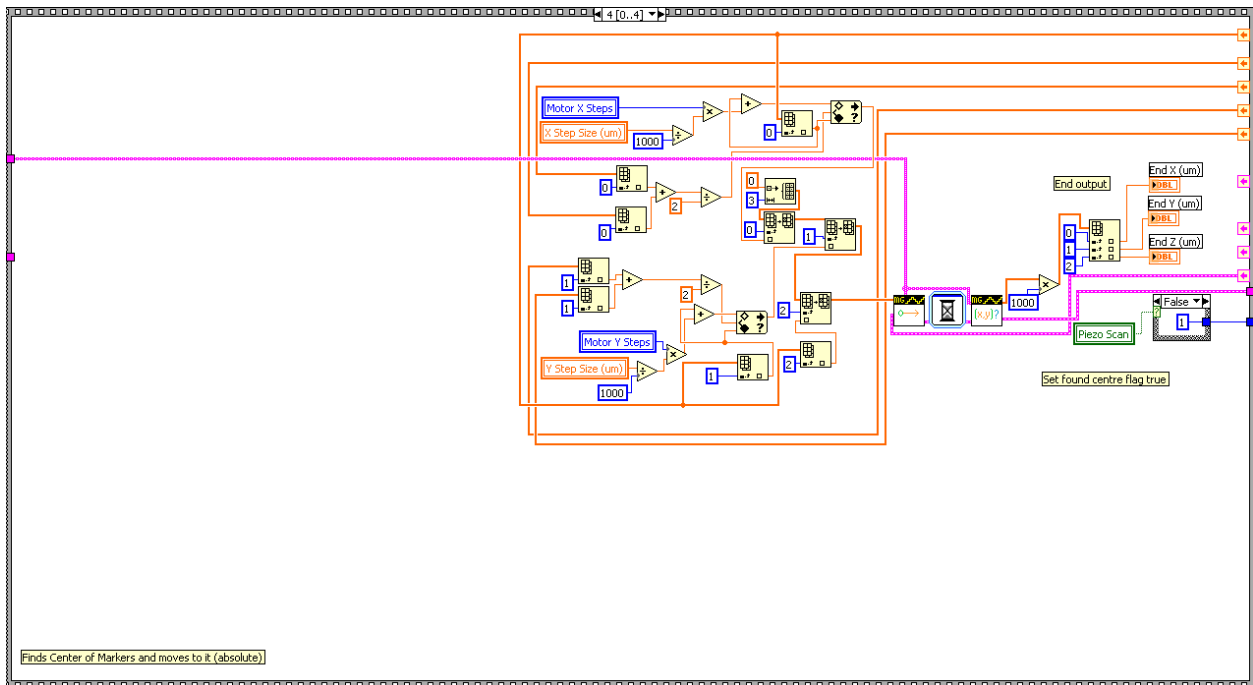

Figure 29: Center finding algorithm stage 5 and 6: Move to reference marker center
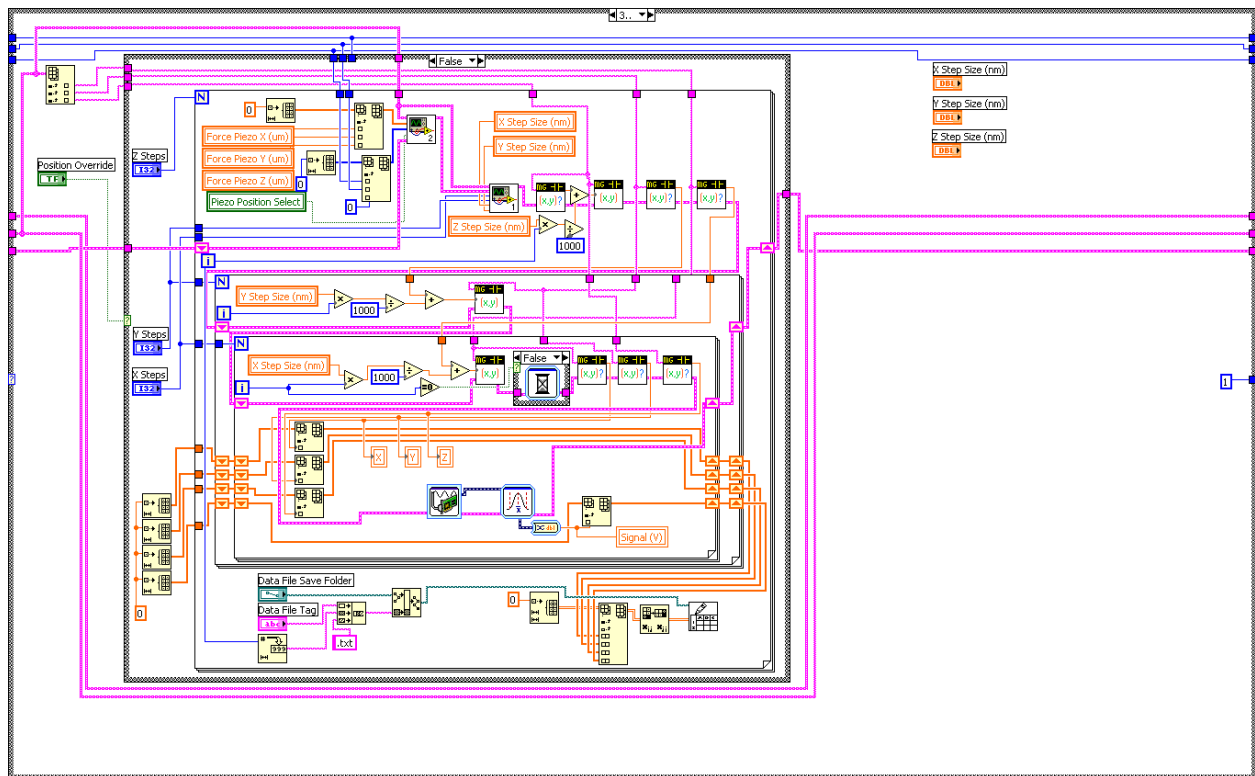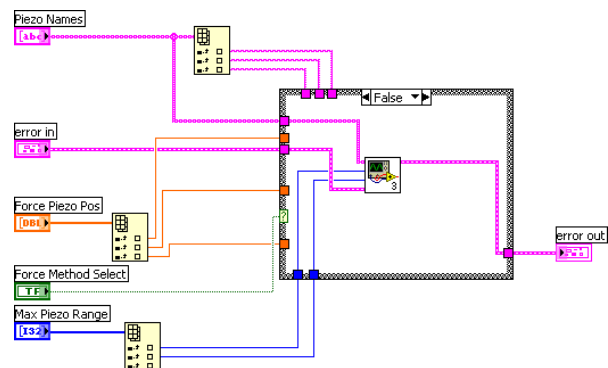
Figure 30: Piezo actuator scanning algorithm

Figure 31: Force piezo to position function

Figure 32: Move to piezo center function

Appendix E MATLAB Code

Plotting Functions

The following MATLAB code was used to process the data files and create the plots seen in this document.

```matlab
function [Dout] = plot_data_mesh( file_name, sx, sy, incr )

    S = load(file_name);
    x = S(:,1);
    y = S(:,2);
    z = S(:,4);


    D = convert_to_matrix(z, sx, sy);
    % Get actual size of matrix
    [sy_actual sx_actual] = size(D);

    surf(0:incr:sx_actual*incr-incr, 0:incr:sy_actual*incr-incr,
smooth_data(D));
    xlabel('X (um)', 'fontsize', 14);
    ylabel('Y (um)', 'fontsize', 14);
    zlabel('Voltage (V)', 'fontsize', 14);
    set(gca, 'FontSize', 14);
    colorbar;
    Dout = D;
end


function [ Dout ] = smooth_data( Din )

% Smooths the data by averaging the average data points around each data
% point
    [sx, sy] = size(Din);
    Dout = zeros(sx,sy);
    for i = 1:sx
        for j = 1:sy
            value = Din(i,j);
            num_samples = 1;
            if i-1 > 0
                value = value + Din(i-1, j);
                num_samples = num_samples + 1;
            end
            if i+1 < sx+1
                value = value + Din(i+1,j);
                num_samples = num_samples + 1;
            end
            if j-1 > 0
                value = value + Din(i, j-1);
                num_samples = num_samples + 1;
            end
            if j+1 < sy+1
                value = value + Din(i, j+1);
                num_samples = num_samples + 1;
            end;
            Dout(i,j) = value / num_samples;
```

```
                end
        end

end

function [ D ] = convert_to_matrix( z, nx, ny )

% Puts the data points in the file into a matrix

    D = 0;
    for i = 1:ny-2
        for j = 1:nx
            D(i,j) = z(((i-1)*nx)+j);
        end
    end
end
```

The following MATLAB code was used to simulate the center finding algorithm on the data in Figure 10.

```
S = load(file_name);
x = S(:,1);
y = S(:,2);
z = S(:,4);

D = 0;
for i = 1:68
    for j = 1:70
        D(i,j) = z(((i-1)*70)+j);
    end
end

thres = 0.5;

sz = size(D);
for i = 1:sz(1)
    for j = 1:sz(2)
        if D(i,j) < thres
            low_row = i;
        end
    end
end

for i = 1:sz(2)
    for j = 1:sz(1)
        if D(j,i) < thres
            low_col = i;
        end
    end
end

for i = sz(1):-1:1
    for j = sz(2):-1:1
        if D(i,j) < thres
            high_row = i;
        end
```

```
        end
end

for i = sz(2):-1:1
    for j = sz(1):-1:1
        if D(j,i) < thres
            high_col = i;
        end
    end
end

middle_row = floor((high_row-low_row)/2+low_row);
middle_col = floor((high_col-low_col)/2+low_col);

D(middle_row, middle_col) = 0;
surf(0:2:138, 0:2:134,D);
```

References

G. Wrigge, J. H. (2008). Exploring the Limits of Single Emitter Detection in Fluorescence and Extinction. *Optical Society of America, 16* (22).

Steckel, J. Advanced Materials 15 (21) 1862 (2003)

Bonadeo, N. H. Science Mag. 282 1473-1476 (1998)

Clough, Young (2011). A study of the development of equipment to be used with the study of quantum dots.

LabVIEW Resources - http://sine.ni.com/psp/app/doc/p/id/psp---357

Optical Systems - http://www.microscopyu.com/articles/optics/index.html

Melles Griot NanoMax TS and Melles Griot 17DRV001 User Manuals